

International Atomic Energy Agency

INDC(GCP)-352
Distrib.: G

INDC

INTERNATIONAL NUCLEAR DATA COMMITTEE

Nuclear Data for Science and Technology

Five papers from U.S.S.R. authors

A.B. Pashchenko and H.D. Lemmel (editors)

July 1993

IAEA NUCLEAR DATA SECTION, WAGRAMERSTRASSE 5, A-1400 VIENNA

Reproduced by the IAEA in Austria
July 1993

Nuclear Data for Science and Technology

Five papers from U.S.S.R. authors

A.B. Pashchenko and H.D. Lemmel (editors)

Abstract:

This report contains five papers on the following topics:

1. **New Nuclear Data Set ABBN-90 and its Testing on Macroscopic Experiments.**
2. **Neutron Cross Sections for Nuclides of Structural Materials.**
3. **The Secondary Neutrons Spectra of ^{235}U , ^{238}U for Incident Energy Range 1 - 2.5 MeV.**
4. **New Data on Prefission Neutrons from 14.7 MeV Neutron-Induced Fission.**
5. **Rotational Modes Contribution to the Observed Level Density.**

July 1993

Table of Contents

Introduction

1. **New Nuclear Data Set ABBN-90 and its Testing on Macroscopic Experiments;**
by V.N. Kosh'cheev, G.N. Manturov, M.N. Nikolaev, A.A. Rineyskiy, V.V. Sinitza, A.M. Tsyboolya and S.V. Zabrodsкая,
Institute of Physics and Power Engineering, Obninsk, The Russian Federation.
2. **Neutron Cross Sections for Nuclides of Structural Materials;**
by M.V. Pasechnik, I.A. Korzh, V.A. Mishchenko, N.M. Pravdivy and N.T. Sklyar,
Institute for Nuclear Research of the Ukrainian Academy of Sciences, Kiev, Ukraine.
3. **The Secondary Neutrons Spectra of ^{235}U , ^{238}U for Incident Energy Range 1 - 2.5 MeV;**
by N.V. Kornilov, A.B. Kagalenko, A.V. Balitsky, V.Ja. Baryba, P.A. Andoresenko and A.A. Androsenko,
Institute of Physics and Power Engineering, Obninsk, The Russian Federation.
4. **New Data on Prefission Neutrons from 14.7 MeV Neutron-Induced Fission;**
by G.S. Boykov and V.D. Dmitriev,
V.G. Khlopin Radium Institute, St. Petersburg, The Russian Federation and
G.A. Kudyaev, Yu.B. Ostapenko, M.I. Svirin and G.N. Smirenkin,
Institute of Physics and Power Engineering, Obninsk, The Russian Federation.
5. **Rotational Modes Contribution to the Observed Level Density;**
by E.M. Rastopchin, M.I. Svirin and G.N. Smirenkin,
Institute of Physics and Power Engineering, Obninsk, The Russian Federation.

Introduction

Attached are five papers by U.S.S.R. authors that were submitted for the Proceedings of the International Conference on Nuclear Data for Science and Technology held from 13 to 17 May 1991 at Jülich, Germany.

The International Programme Committee had decided that only those contributed papers should be considered for publication which have been presented and defended during the conference by one of the coauthors. Since the authors were unable to participate in the Conference, their papers could not be considered for publication.

The texts are reproduced directly from the authors' manuscripts.

NEW NUCLEAR DATA SET ABBN-90 AND ITS
TESTING ON MACROSCOPIC EXPERIMENTS

V.N.Kosh'cheev, G.N.Manturov, M.N.Nikolaev,
A.A.Rineyskiy, V.V.Sinitza, A.M.Tsyboolya,
S.V.Zabrodskaya

(Institute of Physics and Power Engineering, USSR)

Abstract: The new group constant set ABBN-90 is developed now. It based on the FOND-2 evaluated neutron data library processed with the code GRUCON. Some results of the testing ABBN-90 set in different macroscopic experiments are presented.

(ABBN-90, group constant set, FOND-2, evaluated neutron data, testing, macroscopic experiments, code: GRUCON)

ENDF/B type libraries now are the main nuclear data storages recommended for practical applications. There is such library in the USSR also /1/. But multigroup method monopolistically used in the engineering calculation practice as before and thus maintainance of the group constant set by no means lost its importance with developing of evaluated nuclear data libraries.

Group constant set ABBN /2,3/ widely used in the USSR for the different reactor and shielding calculations and for other applications connected with the neutron and photon fields calculations. A new version of this group constant set ABBN-90 with more wide possibilities is developed now. Neutron data in this set were calculated on the basis of FOND-2 library /1/ with the code GRUCON /4/. Thus data for almost all stable materials, for all important actinids and fission products were included in this constant set.

The main group structure conserves as previous - the same 28 groups from (-1)-st to 26-th (thermal) /2/. But for the important reactor materials the data for several fine groups are given in groups with strong energy dependence of cross sections. The number of such fine groups may be as much as 12. The fine group divisions are sufficient for description with acceptable accuracy of the smooth cross sections in the fast neutron region (in the case of hydrogen for example), for description of cross section behavior in the vicinity of strong s-resonances as such materials as sodium, iron, uranium-238 etc, and for description of thermalization phenomena. Unresolved resonance structure is described with the help of Bondarenko factors as well as by subgroup approximation. In the last case subgroup parameters are constructed by such a manner that only subgroup cross sections are temperature dependent. Because subgroup parts are temperature independent the ABBN-90 constant set may be used for all calculations when temperature gradient must be taken into account.

A special text format is developed for computer representation of ABBN constants. It is maximally convenient for visually data control (data presented in the headed columns in the fixed point form etc). The edition of the data by users is very easy.

The ABBN-90 constant set includes the data of the next types:

- main neutron constants (total, capture, fission, elastic and inelastic scattering cross sections, σ , μ , ξ);
- inelastic scattering intergroup transfer matrices (probabilities and average cosines);
- elastic scattering intergroup transfer matrices (to 5-th angular momentum including);
- resonance selfshielding factors;
- its Doppler increments;
- subgroup resonance structure parameters;
- neutron reaction cross sections;
- KERMA- factors;
- delayed neutron data;
- neutron reaction photon production data (15 photon groups);
- photon interaction data;
- fission products yields;
- decay data for radionuclides produced in the neutron reactions;
- radioactive decay photon spectra(15 groups and 4 strongest discret lines).

Computer code CONSYST processed the ABBN-90 constants to the forms needed for calculational codes.

Testing of ABBN-90 constants on the banchmark macroscopic experiments stored in the INDEKS library /5/ is fulfilled now.

The first group of such experiments is the criticality data for uranium and plutonium fueled critical assemblies with different hardness of neutron spectra.

As must be waited differencies between experimental and calculational data to be found greater that in the case when previous constant set version ABBN-78 (adjusted to the best agreement with these experiments) was used (see Table 1). In the case ABBN-90 it was decided the adjustment would be fulfilled not on the level of the group constants but on the level of evaluated data files. This work is only began now. So it was investigated for example the dependence of k_{eff} calculational inaccuracy from the blanket thickness of hard uranium and plutonium fueled critical assemblies when different version of evaluated data was used (Fig.1). It was found that using of ENDF/B-6 ^{235}U data allowed to discribe the criticalities with better accuracy than it is doing with using ABBN-78 or ABBN-90 constant sets. Further, the analysis of descreapancies between many threshold reaction cross section ratios measured in the centra of the hard critical assemblies cores had show that these descreapancies may be essentially reduced if fission neutron spectrum would be adopted more hard than in ABBN-90. In particularly this

analysis give arguments in favour of the neutron spectrum induced by the ^{235}U thermal neutron fissions adopted in ENDF/B-5. The average energy of this spectrum as high as 2.03 MeV is confirmed apparently only in one experiment /6/. Fission spectrum with average energy 1.98 MeV is adopted now in ABBN-90. This value is followed from averaging of the data of many authors .

The conclusion that E is greater than 2 MeV is confirmed and by the data of the second group of experiments considered by us: measurements of different reaction cross sections in fission neutron spectra.

The third group of experiments attracted to ABBN-90 constant set testing are the experiment on the critical assemblies with the insertions with $k_{\text{eff}} \approx 1$. Data of SCHERZO-S.56 /7/ and other similar experiments in particular with UO_2 feeding by the fissions of ^{235}U or ^{239}Pu allow to test the ^{235}U capture and inelastic scattering cross sections. Previous conclusion /8/ about necessity of reducing of ^{235}U σ_{in} in hundreds keV region relatively data of /8,9/ is conserved till now and was confirmed experimentally /10,11/. The conclusion about necessity of reducing of ^{235}U σ_{in} /8/ also find the confirmation in the experiments /12/. In the more later experiments was founded more lower values of ^{235}U capture cross sections /13/ which was indirectly confirmed by the simultaneously evaluation of the capture, elastic and inelastic scattering cross sections and of the flat and capture self-indication transmission data /14/. The authors of ref. /15/ came to the similar conclusions despite of deep transmission data were not attracted to analysis.

Measured transmission curves, the fourth group of experiments, allow to essentially increase the availability of resonance self-shielding factor calculations on the basis of the evaluated neutron data files.

The data for structure materials had tested on the basis of the COBRA facility experiments /16/. Discrepancies between calculations and measurement of k^* and reactivity ratios in the media with Cr, Fe and Ni with $k_{\text{eff}} \approx 1$ showed on Fig.2.

It is easy to see that iron constants calculated on the basis of libraries FOND-2 and ENDF/B-6 lead to the practically coincident results, ENDF/B-6 based nickel constants are better than those based on FOND-2 (but only if failed low energy ^{63}Ni resonance parameters are introduced in the ENDF/B-6 data). In the case of chromium the FOND-2 data are preferable. Let us pointed out that the data on fission neutron removal cross sections (under the ^{235}U fission threshold) for iron, nickel and chromium calculated from FOND-2 and ENDF/B-6 data are in the agreement with each other and with the results of fifth group of experiments - measurements of fission neutron spherical transmission /16/.

The sixth group of experiments attracted to ABBN-90 data testing were transmutation experiments fulfilled on the BN-350 and BN-600 reactors. Some data from this very extensive experiments are listed in the Table 2 in

Table 1.

The ratios C/E using ABBN-78 and ABBN-90

| assemble | k_{eff} | | f8/f5 | | f9/f5 | | c8/f5 | |
|--------------|-----------|------|-------|------|-------|------|-------|------|
| | 78 | 90 | 78 | 90 | 78 | 90 | 78 | 90 |
| SCHERZO-5.56 | -1.5 | -0.4 | 2.2 | 2.0 | 2.4 | 0.4 | 1.3 | 0.5 |
| BIG-TEN | -0.2 | 0.6 | -1.1 | -1.3 | 0.0 | -1.9 | 0.0 | -1.5 |
| ZPR-3-12 | 0.0 | 1.0 | -0.2 | 0.0 | 0.0 | -1.8 | -0.1 | -0.8 |
| ZPR-6-6A | -0.1 | 1.7 | -8.6 | -6.4 | - | - | - | - |
| ZPR-3-48 | 0.0 | -0.8 | -3.4 | 0.2 | 0.1 | -0.5 | -2.9 | -1.8 |
| ZPR-3-53 | -0.6 | -1.0 | 5.1 | 11.1 | -10.5 | -7.7 | - | - |
| ZPR-6-7 | -0.3 | -1.4 | -8.5 | -4.9 | -4.3 | -5.2 | 1.4 | 3.4 |
| ZPPR-2 | -0.2 | -1.5 | 2.0 | 6.2 | -1.8 | -2.9 | - | - |

Table 2.

The ratios C/E for BN-350 reactor using ABBN-78 and ABBN-90

| index | ABBN-78 | | | ABBN-90 | | |
|------------|---------|--------|---------|---------|--------|---------|
| | core 1 | core 2 | core PU | core 1 | core 2 | core PU |
| C8/f5 | 1.00 | 1.01 | 0.99 | 1.00 | 1.01 | 1.00 |
| f8/f5 | 1.01 | 0.98 | 0.97 | 1.04 | 1.01 | 1.01 |
| f9/f5 | 1.01 | 1.00 | 0.99 | 0.99 | 0.98 | 0.98 |
| α_5 | 0.99 | 1.09 | - | 0.94 | 1.04 | - |
| α_9 | 0.98 | - | 0.99 | 1.09 | - | 1.05 |

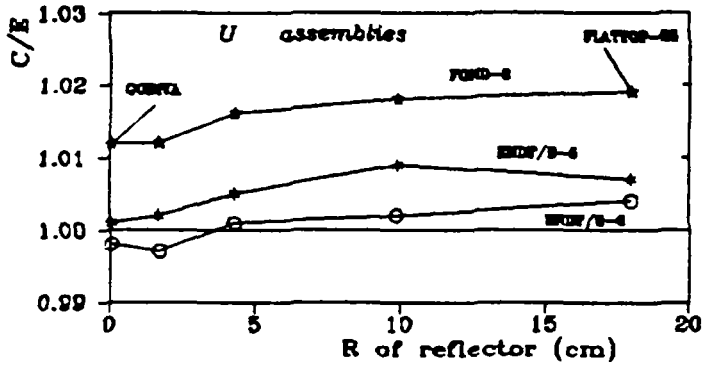
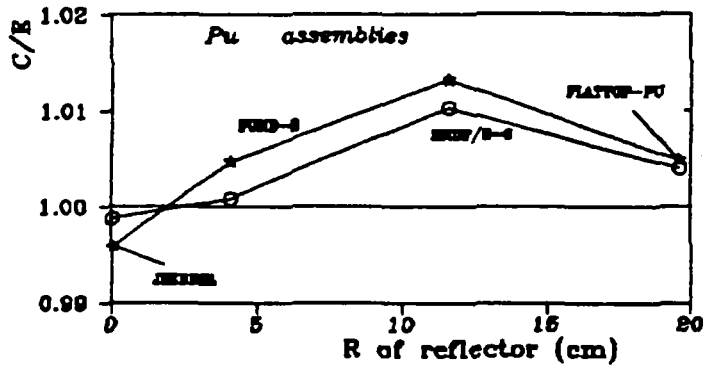


Fig.1. The C/E of k-eff values for spherical metallic systems

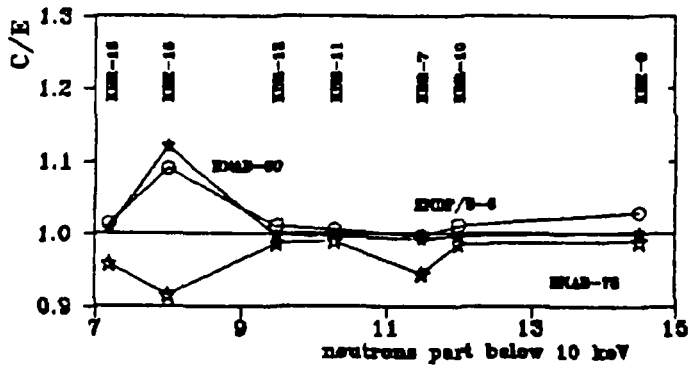


Fig.2. The C/E of k+ values for COBRA experiments

comparison with calculated data. Let us point out that ENDF/B-6 based constants were used only for reaction rate calculations by the averaging over the spectra calculated by ABBN-90 constants.

ABBN-90 constant set was used also for calculational analysis of critical experiments with the tight uranium-water and uranium-plutonium-water lattices. Fully successful results were received.

The testing of ABBN-90 constant set is continued.

References

1. Elohin A.I., Ignatuk A.V., Kuznetsov B.D., Koshichev V.N. et al. The library of evaluated data. This conference. Julich, may, 1991.
2. Abagyan L.P., Bazazyants N.O., Bondarenko I.I., Nikolaev M.N. Group Constant for Nuclear Reactor Calculations. - N.Y., Consultants Bureau, 1964.
3. Abagyan L.P., Bazazyants N.O., Nikolaev M.N., Tsyboolya A.M. The group constants for reactor and shielding calculation. Energoizdat, 1981.
4. Sinitza V.V. VANT, issue: Nuclear Constants, 1984, v.5, p.74.
5. Manturov G.N. VANT, issue: Nuclear Constants, 1984, v.5(59), p.20.
6. Johansson P.I. Nucl. Sci. and Eng., 1977, v.62(4), p.695.
7. Chaudat J.P., Darrouzet M., Fisher E.A. Experiment in Pure Uranium Lattices with Unit k_{∞} Assemblies: SNF91-3187, UF1 and UK5 in ERMINE and HARMONIE. KFK-1865(CEA-R-4552), 1974.
8. Barnard E. et al. - Proc.Conf. on Nuclear Data for Reactors, IAEA, Vienna, v.2, 1970, p.103.
9. Guenther P., Smith A. - Proc.Conf. on Nuclear Cross Sections and Technology, Washington, NBS, 1975, v.2, p.700.
10. Tsang F.Y., Brugger R.M. Nucl. Sci. and Eng., 1978, v.65, p.70.
11. Litvinskiy L.L., Vertebniy V.P. et al. Atomnaya energiya, USSR, 1987, v.62(3), p.192.
12. Katakov L.E., Kononov V.N. et al. VANT, issue: Nuclear Constants, v.3, 1986, p.37.
13. Adamchik U.V., Voskonyan M.Y. et al. - Atomnaya energiya, v.65(5), 1988, p.356.
14. Georgiev G.P., Grigoryev U.V. et al. Measurement and Analysis of Resonance Structure of the ^{238}U total and radiative capture cross sections in the energy region 0.465-200 keV. This conference. Julich, may, 1991.
15. Frohner F.H. - Nucl. Sci. and Eng., 1989, v.103, p.119.
16. Nikolaev M.N. et al. - Proc.Conf. on Nuclear Data for Science and Technology, Mito, 1988, p.615.

NEUTRON CROSS SECTIONS FOR NUCLIDES OF STRUCTURAL MATERIALS

M.V.Pasechnik, I.A.Korzha, V.A.Mishchenko, N.M.Pravdivy and
N.T.Sklyar

Institute for Nuclear Research of the Ukrainian Academy
of Sciences, Kiev, Ukrainian SSR

Abstract. Differential and integral cross sections of neutron elastic and inelastic scattering from the structural material nuclides titanium-48, chromium-50,52,54, iron-54,56, nickel-58,60,62,64 and molybdenum-92,94,96,98 are measured in the energy range 1.5-7.0 MeV and analysed in the energy range 1.0-9.0 MeV together with other authors' data using spherical optical model, coupled channel method and statistical model. As an example, typical results for molybdenum-96 are presented. Relative contributions of the direct and compound mechanisms to the scattering cross sections are determined.

(fast neutrons, ^{48}Ti , $^{50,52,54}\text{Cr}$, $^{54,56}\text{Fe}$, $^{58,60,62,64}\text{Ni}$, $^{92,94,96,98}\text{Mo}$ targets, time-of-flight spectrometer, differential cross sections, integral cross sections, elastic scattering, inelastic scattering, optical models, coupled channel theory, statistical models, comparative evaluations, direct reactions, compound-nucleus reactions)

Introduction

The role of structural materials in nuclear technology is important and becomes still more important in the last years because of strengthening the attention to secure functioning of the nuclear installations. Moreover, most of the structural materials consist mainly of the spherical even-even nuclides, forming a nuclide class with characteristic properties, which are evidently interesting also from theoretical point of view. This nuclide class is a constant object for experimental and theoretical investigations, but a vast field for activity in widening and correcting the existing data base remains.

In order to contribute to solution of the above problems we have carried out a cycle of measurements the neutron elastic and inelastic scattering cross sections for the structural material nuclides and their theoretical analysis using an optical-statistical approach. The results are partly published (e.g., /1-3/); they are presented here in a generalized form and illustrated with new data for molybdenum-96.

Experimental procedure

The differential cross sections of neutron elastic and inelastic scattering were measured using the modernized version of the fast neutron time-of-flight spectrometer at the electrostatic accelerator EG-5 /4/. The monoenergetic neutrons in the energy range 1-7 MeV with the energy spreads $\pm(50-170)$ keV were produced in the reactions $T(p,n)$ or $D(d,n)$ using solid targets Ti-T or Ti-D. In the measurements cylindrical highly enriched (> 90 %) isotopic samples, having masses 30-150 grams were used. The

scattered neutron spectra, were measured in the angle range 20-150° at the flight distances 1.5-2.8 m in relative good background conditions. The experimental apparatus and procedure are described in detail in the paper /4/.

Experimental results

Differential cross sections of neutron elastic scattering and inelastic scattering with excitation of one-to-five lowest discrete levels or level groups of titanium-48, chromium-50,52,54, iron-54,56, nickel-58,60,62,64 and molybdenum-92,94,96,98 were measured in the energy range 1.0-7.0 MeV. The measured cross sections were corrected for neutron flux attenuation and multiple scattering in the sample and for the geometrical factors. The total errors of the differential cross sections are mainly 3-10 % for the elastic scattering and 5-12 % for the inelastic scattering and include the measuring, normalizing and correction errors.

A comparison of our measured differential cross sections with the existing in the literature other authors' data has shown that a great part of the cross sections at the investigated energies are obtained only by us and the rest of our data are, on the whole, in good agreement with the data of other authors at comparable neutron energies. Our data essentially supplement and make more precise the data base on cross sections of neutron elastic and inelastic scattering from nuclides of structural materials.

As an example, the measured differential cross sections of neutron elastic and inelastic scatterings from molybdenum-96 in the energy range 1.4-5.0 MeV are presented in Fig.1 in which, for comparison, the data of other authors at

comparable energies obtained for monoisotope samples in analogous procedure /5-7/ are given. It is evident from the Figure, that a comparison may be performed only at the energy 1.4 MeV. The elastic scattering cross sections at the energy 1.4 MeV are in a good agreement with the cross sections of the paper /5/ at the same energy, and the data of the paper /6/ at the energy 1.5 MeV are slightly, but conformably different from the both data sets at the energy 1.4 MeV. In our experiments the inelastic scattering cross sections at excitation of five lowest levels in molybdenum-96 (level energy in keV) 778 (2^+), 1148 (0^+) and 1498 (2^+)+1626 (2^+)+1628 (4^+) were measured. The cross sections measured at the energy 1.4 MeV may be compared with the data of the paper /5/ at the same energy and of the paper /6/ at the energy 1.5 MeV. On the whole, an agreement among the data is satisfactory.

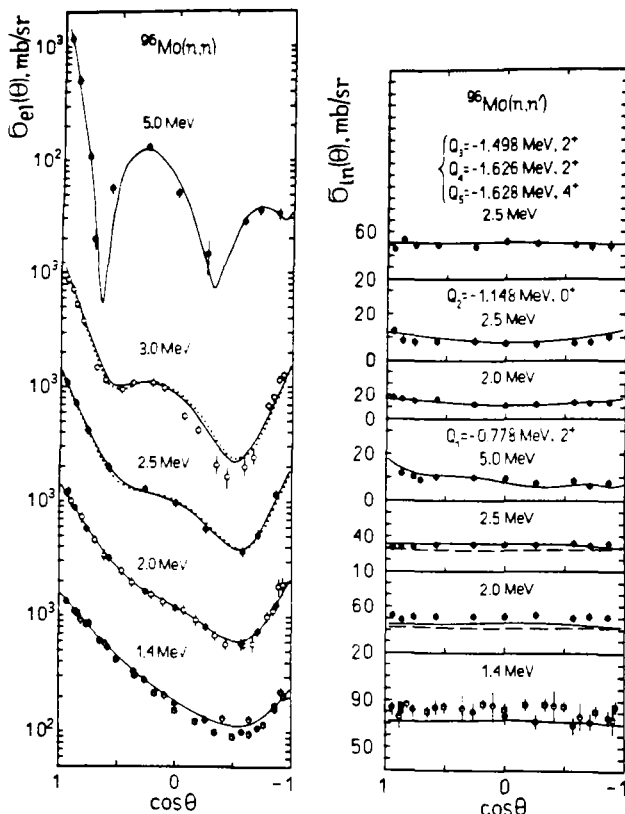


Fig.1. Differential cross sections of neutron elastic and inelastic scatterings from molybdenum-96. The experimental data: ● - this work, ○ - /5/, ■ - /6/, □ - /7/. The curves are results of the model calculations of the cross sections: elastic - OM+SM (solid), CC+SM (dotted) and inelastic- CC+SM (solid), SM (dashed).

The integral cross sections of the elastic and inelastic neutron scatterings were obtained by angular integration of the measured differential cross sections. Moreover, inelastic scattering cross sections near the excitation thresholds of the first 2^+ levels of the nuclides iron-

56 and molybdenum-94,96,98 (0.9-1.4 MeV) are obtained using registration of gamma-radiation from the reaction $(n,n'\gamma)$ with Ge(Li) spectrometer. The obtained integral elastic scattering cross sections, on the whole, are in satisfactory agreement with the existing other authors' data in the energy range 1.0-9.0 MeV. The integral inelastic scattering cross sections are also, on the whole, in an agreement with the other authors' data, but also essential disagreements, particularly near the excitation thresholds of the levels, are observed.

The degree of such an agreement may be evaluated in Fig.2 which shows our data and other authors' data on integral cross sections of elastic and inelastic scattering of neutrons in the energy range 1.0-9.0 MeV from molybdenum-96 /5-8/ and molybdenum of natural isotope composition (for elastic scattering) /9-12/. It may be seen from the Figure that our elastic scattering data and these of other authors are in a good agreement. The first 2^+ level excitation cross sections generally are in a good agreement, except the energy range near the level excitation threshold, where the data were obtained using a gamma-spectrometry method. Our data and these of other authors for the second level, as well as for the sum of the third-to-fifth levels are in a sufficiently good agreement.

Theoretical analysis

The measured cross sections together with the other authors' data on total cross sections and scattering cross sections in the energy range 1.0-9.0 MeV were analysed using a spherical optical model (OM), coupled channel method (CC) and modern versions of statistical model (SM). Procedures of such analyses were described in the paper /13/. In the optical model calculations a set of averaged optical potential parameters, which we have determined in earlier detailed analyses, as well as several existing in the literature optimized parameter sets were used. In the CC-calculations the same potential parameters, as in OM, except the absorption potential, which was taken $0.8W_{OM}$ (for two-channel coupling version) or $0.7W_{OM}$ (for five-channel coupling version), were used. In the statistical model calculations up to energies 3.0-4.8 MeV were accounted discrete levels with known characteristics and contributions of higher levels with unknown characteristics were accounted using a Fermi-gas model with "back-shift" and parameters from the papers /14/.

Comparison of the so calculated theoretical cross sections with the experimental ones has shown that under correct accounting the direct and compound scattering mechanisms, even by using the averaged parameters of optical potential, it is possible to obtain a satisfactory agreement of the theoretical total cross sections and differential and integral cross sections of elastic

and inelastic scatterings of 1.0-9.0 MeV neutrons from nuclides of structural materials with the experimental data.

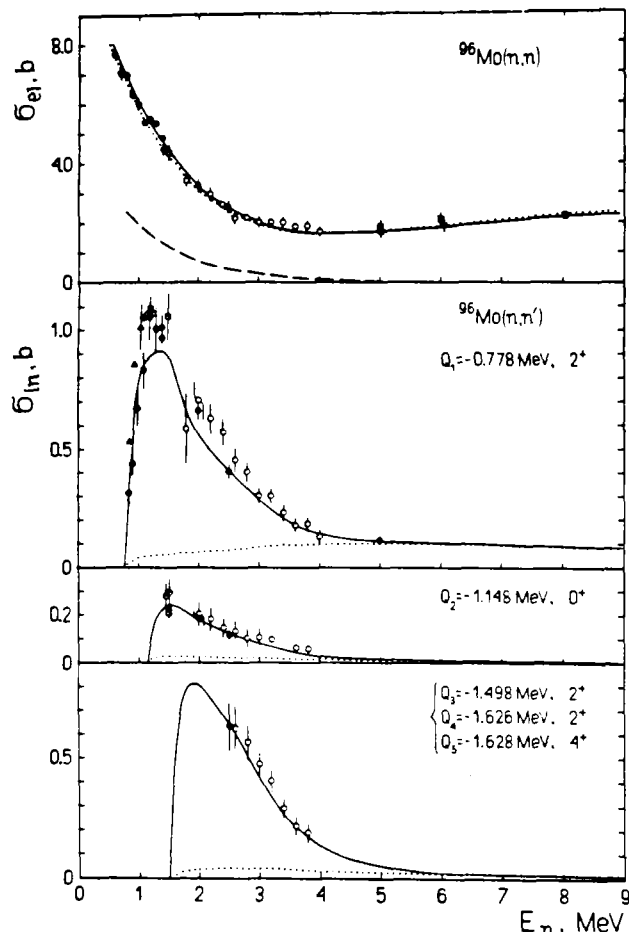


Fig.2. Integral cross sections of neutron elastic and inelastic scatterings from molybdenum-96. The experimental data: ● - this work, ○ - /5/, ■ - /6/, ◦ - /7/, △ - /8/, □ - /9/, ▽ - /10/, ▣ - /11/, ▤ - /12/. The curves are the results of the model calculations of the cross sections: elastic - $OM+SM$ (solid), $CC+SM$ (dotted), SM (dashed) and inelastic - $CC+SM$ (solid), CC (dotted).

As an example, in Figs.1 and 2 the theoretical cross sections of the neutron scatterings from molybdenum-96 in comparison with the experimental data are presented. It may be seen from the Figures that both differential and integral theoretical cross sections are in sufficiently good agreement with the experimental ones. Such an agreement is a reason for practical applications of the calculation results instead of experimental data, if they are absent.

Adequate theoretical description of the experimental cross sections of neutron scatterings from the nuclides under investigation gave a possibility to make reliable evaluations of relative roles of the scattering mechanisms (direct and compound) and their changes with the incident neutron energy change /15/. For

example, the cross sections of direct excitation of the first 2^+ levels at the incident neutron energies ~ 1 MeV above the excitation thresholds doesn't exceed 15 percents of the summed cross sections and to the end of the used energy range becomes dominant. The two-phonon triplet levels of the nuclides under investigation in a large energy range are excited predominantly through compound nucleus formation and only to the ends of the energy and mass ranges contributions of the direct mechanism to the cross sections of their excitations become also dominant.

References

1. I.A.Korzh, V.A.Mishchenko, M.V.Pasechnik and N.M.Pravdivy, in Nucl. Data for Sci.and Technol., Proc.Int. Conf., 1982, Antwerpen, Belgium, p.159, D.Reidel Publ.Co., Dordrecht e.a. (1983).
2. И.А.Корж, в кн. Нейтронная физика, Материалы 6-ой Всес.конф.по нейтрон. физ., 1983, Киев, СССР, т.3, с.99, ЦНИИатоминформ, Москва (1984).
3. И.А.Корж, В.А.Мищенко и Н.М.Правдивый: Атомная энергия 62, 417 (1987).
4. И.А.Корж, В.А.Мищенко и И.Е.Санжур: Укр.физ.журн. 25, 109 (1980).
5. F.Lambropoulos, P.Guenther, A.Smith and J.Whalen:Nucl.Phys. A201,1(1973).
6. F.D.McDaniel, J.D.Brandenberger, G.P.Glasgow and H.G.Leighton: Phys. Rev. C10, 1087 (1974).
7. A.B.Smith, P.Guenther and J.Whalen: Nucl.Phys. A244, 213 (1975).
8. Е.С.Конобеевский, Р.М.Мусаелян, В.И.Попов и И.В.Суркова: Физика элем. част.и атом.ядра 13, 300 (1982).
9. R.W.Hill: Phys.Rev. 109, 2105 (1958).
10. R.M.Wilenzick, K.K.Seth, P.R.Bevington and H.W.Lewis: Nucl.Phys. 62, 511 (1965).
11. B.Holmqvist and T.Wiedling, Optical Model Analyses of Experimental Fast Neutron Elastic Scattering Data, AE-430, Aktiebolaget Atomenergie, Studsvik (1971).
12. M.T.McEllistrem, in Proc.Int.Conf.on Interact. of Neutrons with Nuclei, 1976, Lowell, USA,(ed.by E.Sheldon), v.1, p.171, Lowell Univ., Lowell, (1976).
13. И.Корж, В.П.Дунев, В.А.Мищенко, Э.Н.Можухин,Н.М.Правдивый и Е.Ш.Суховицкий: Вопр.атом.науки и техники, сер.Ядер.конст.вып.1(50), 40 (1983).
14. W.Dilg,W.Schantl, H.Vonach and H.Uhl: Nucl.Phys. A127, 269 (1972); В.М.Бычков, О.Т.Грудзевич и В.И.Пляскин: Вопр.атом.науки и техники, сер. Ядер. конст. вып.3, 14 (1987).
15. И.А.Корж, в кн. Нейтронная физика, Материалы I Международной конф. по нейтрон.физ., 1987, Киев, СССР, т.3, с.136, ЦНИИатоминформ, Москва (1988).

THE SECONDARY NEUTRONS SPECTRA OF ^{235}U , ^{238}U
FOR INCIDENT ENERGY RANGE 1 - 2.5 MeV

N. V. Kornilov, A. B. Kagalenko, A. V. Balitsky, V. Ja. Baryba, P. A. Androsenko, A. A. Androsenko

Institute of Physics and Power Engineering, Obninsk, USSR

Abstract. Spectra of inelastic scattered neutrons and fission neutrons were measured with neutron time of flight spectrometer. The solid tritium target was used as a neutron source. The energy distribution of neutrons on the sample was calculated with Monte-Carlo code, taking into account interaction in the target and reaction kinematics. The detector efficiency was determined with ^{252}Cf source. The multiple scattering and absorption corrections were calculated with codes packet BRAND. Our results confirm ENDF/B-6 data library.

(^{235}U , ^{238}U , neutrons, elastic and inelastic scattering, fission neutrons, multiple scattering and absorption corrections, Monte-Carlo code, ENDF/B-6 data library)

INTRODUCTION

The requirement for measuring differential cross-section of inelastic neutron scattering on fissile elements nuclei in the MeV-energy range primarily resulted from the needs of atomic power engineering. These demands can hardly be considered satisfactory. In a number of cases the difference between latest experiments [1] and the evaluation data amounts to 30-50%. In new estimates for ^{235}U [2] the inelastic scattering cross-section increased ~1.5 times as compared with ENDF/B-5 library that requires an additional substantiation. There are discrepancies between evaluations [2] and ENDF/B-6 in 1-2 MeV energy range.

An investigation of inelastic fissile scattering cross-section entails a number of methodical problems. A high density of low states allow no reliable measurements of scattering cross-section on individual levels and distinguish of contribution of elastic scattering. In addition, the neutrons spectra measured are restricted at low energy by the energy 200-500 keV due to detection threshold. These features hinder the measurements of total inelastic cross-section and the comparison of experimental data. These problems were basically settled in [1] where the "pseudo-elastic" scattering cross-section was measured for a number of fissile nuclei. In this study a conclusion was made that for ^{232}Th , ^{233}U , ^{235}U , ^{238}U total inelastic scattering cross-sections are known with reasonable accuracy and are in good agreement with ENDF/B-5 evaluation, and subsequent refinement is requisite for energy distribution of scattering neutrons on these nuclei.

The above feature have specified the objective of this study: the investigation of inelastic neutron scattering for the refinement of total inelastic scattering cross-section and scattered neutron spectra, for the implementation of the problem set out a particular attention was paid to decreasing the detection threshold to raising the measurement accuracy in the region of low scattered neutron energies, simulation of experiment, taking into account of unmonoenergetic neutrons.

EXPERIMENTAL TECHNIQUE

The neutron spectra were measured by time-of-flight method on the EG-1 accelerator spectrometer at the IPPE. The spectrometer specifications are: pulse width - ~1 ns, repetition rate - 2 MHz, path length - ~2 m, mean current on the target 4-6 μA . The $T(p,n)$ reaction in a solid tritium-scandium target was used as a

neutron source. Ref. [3] describes the neutron spectrometer in more detail. The specification featuring this study are only included below.

Disc-shaped samples 10 mm in thickness and 46.3 mm in diameter fabricated of metallic ^{235}U , ^{238}U were arranged at a distance 9.5 cm from the target. The normal to the sample surface was in "source-sample-detector" plane and turned at the angle -30° against the incident protons direction. The percentage of sample amounted to: 99.5% for ^{238}U , and 89.6% ^{235}U and 10.4% ^{238}U for ^{235}U sample. The sample was packed in Al-container with a wall thickness 0.3 mm.

The neutron detector was a plastic scintillator 80 mm in diameter and 20 mm in thickness. The detector face was coated with lead absorber 2 mm in thickness to reduce the background of inherent gamma-quanta. The detector efficiency (threshold ~60 keV) was measured with respect to ^{252}Cf fission neutron spectrum. The ^{252}Cf source was attached in sample location.

The neutron flux on the sample was measured by scattering on a carbon sample (51 mm diameter, 15 mm thickness) and with respect to ^{235}U fission. In latter case ionization fission chamber, installed between source and sample was used. All spectra were measured at the angle 120° . Each measurement consisted of 10-12 runs with duration about one hour. For each initial neutron energy as many as two measurements were performed on investigated sample. In addition the measurements were made of:

- neutron spectra with an Al-container,
- neutron spectra with C-sample,
- source neutron spectra at the angle 0° .

DATA PROCESSING AND DISCUSSIONS

At the first stage of processing the monitor time-of-flight spectra were applied for accelerator performance quality verification in each run (time resolution, energy stability). The spectra of "good" runs were summed up. The non-correlated background was subtracted from overall spectra. The detector spectrum was measured as two-dimension array (time*amplitude, $512*32$) therefore the zero-effect time interval was known for each amplitude group. Contents of channels in this time intervals was reduced to zero after background subtraction. This procedure resulted in the improvement measurement accuracy in low energy range for neutron spectrum.

The resulting time spectrum was normalized to the "long" counter with the background spectrum measured with Al-container subtracted from it. The time spectrum was transformed into an energy

scale, normalized to obtain absolute cross-section. Corrections were made for detector efficiency and contribution of ^{238}U scattering for ^{235}U samples. In addition the "non-monoenergetic" neutron background obtained from the "direct flux" measurements was subtracted. In this case only elastic scattering was assumed, that is valid due to low value of this background 3-5%.

Corrections for different sample size and its position were calculated using MC code.

The correction for neutron multiple scattering and attenuation in the sample were calculated in Monte-Carlo method using the BRAND code system [4]. The differential cross-section of carbon scattering was taken from [5]. The neutron flux determined from the fission chamber was systematically ~3.5% less than carbon scattering one. Taking into account the accuracy of flux determination in chamber case being lower (5%), the normalization on carbon scattering was subsequently applied. However, the employment of two methods enable us to more realistically estimate the accuracy of data absolutization.

Fig. 1, 2 show the spectra of secondary neutrons (scattering and fission) together with calculation results. It should be emphasized that the calculation presents not only a neutron

interaction in the sample, but simulates the experiment completely: from a source to a detector. The calculations were made in time scale and was transferred into energy scale applying the codes for experimental spectra processing.

The neutron data from NEDAM [8] library only are currently accessible for the BRAND code system. As can be observed in fig. 1, 2 this set of neutron data does not describe the experiment. The correction for multiple scattering and absorption gained from these calculation can in some case essentially distort the experimental results, that is why the neutron spectra were not corrected for this effects. The correction was introduced solely for the integral cross-section where the impact of scattering neutron spectra shape was less significant. A preliminary procedure for including ENDF/B-6 library into calculation is presently underway.

Table 1 show integral cross-section of inelastic scattering. Column 1 give the the initial energy of neutron on a sample and its r.m.s. deviations, column 2 - integration boundaries, column 4 integral cross-sections including part of fission neutrons corrected for the effect of multiple scattering and attenuation. Column 5 show the cross-section with fission neutron contribution subtracted, multiplied by 4π . Column 6, 7 state inelastic scattering cross-section on low energy levels (ENDF/B-6) falling out integration area and total inelastic cross-section. The fission neutron spectrum is assumed

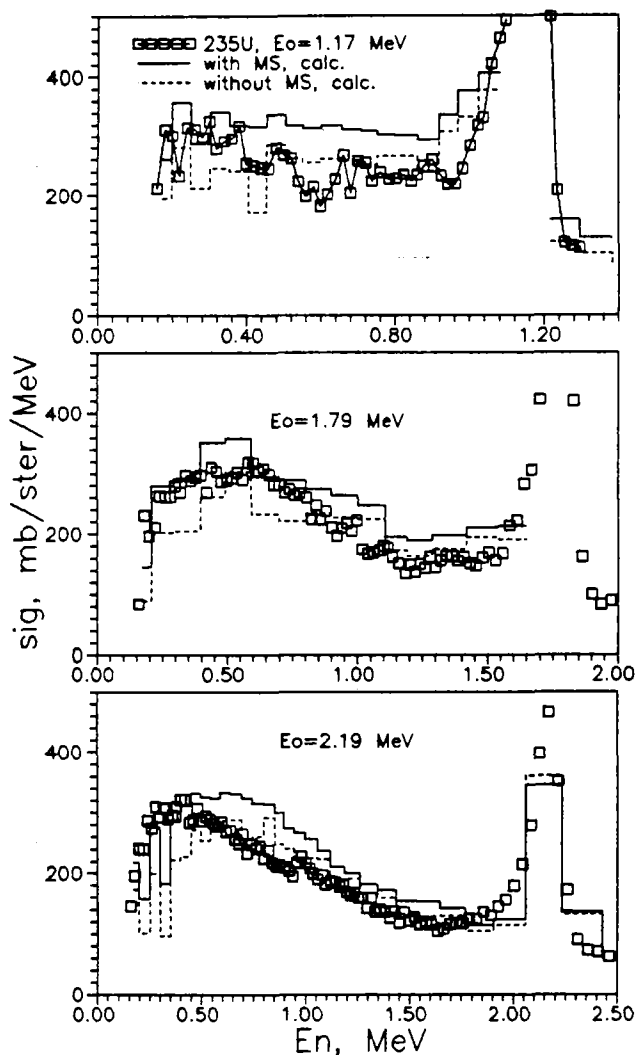


Figure 1. Spectra of scattered neutrons and ^{235}U fission neutrons. Histograms stand for the calculation results without attenuation and MS (dashed line) and taking into account these processes (solid line).

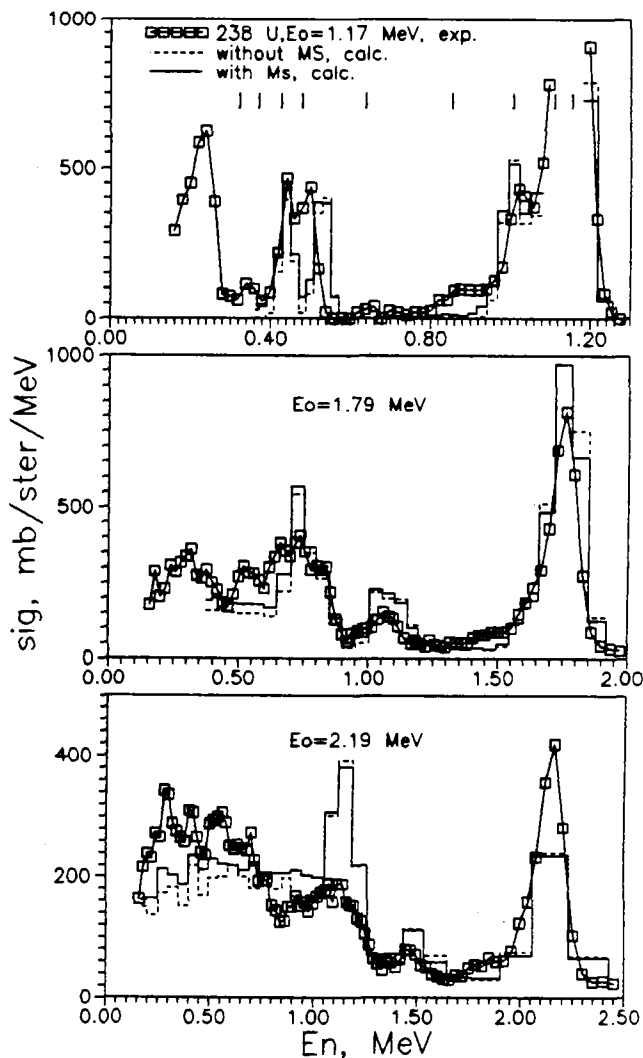


Figure 2. Same neutron spectra for ^{238}U .

to be Maxwell distribution with the "temperature" T_1 , fission neutron have isotropic angular distribution. Fission cross-section are taken from [5], fission neutron spectra temperature - from systematic in [6].

Fig. 3 shows the total cross-section of inelastic scattering by the data of this and other studies together with evaluated cross sections from various libraries.

For ^{238}U a set of levels excluding from experimental cross-section is more unambiguous. As a rule it is the first one or two levels. The cross-sections for this levels from evaluation [9] and ENDF/B-6 agree. The total inelastic cross-section of our study and Ref. [1] are in reasonable agreement, confirm ENDF/B-6 evaluation and are systematically higher evaluation [9].

In ^{235}U case situation is more difficult. We don't know exactly the set of levels. However, by virtue of the scattering cross-sections at individual levels being small, it does not results essential error. The data of this study within the limits of errors agree with the data of Ref. [1] and ENDF/B-6 estimation. The ENDF/B-5 estimations etc. covers the experimental points with the scattering cross-section on low-lying levels not added. In the 1-2 MeV energy range our data and those of Ref. [1] do not confirm the cross-section course put forward in Ref. [2].

We are planning to analyze fission neutron spectra shapes on the base of our data for checking fission neutrons subtraction and calculate multiple scattering correction with ENDF/B-6 library. However, we can made some conclusions now. As can be observed from fig.3 the further investigations of the inelastic scattering cross-section is required for ^{235}U in the energy range (1 MeV with the aim for solving a contradiction between the evaluated cross-sections and data of Ref[1].

The main components of the errors in this experiment are: the accuracy of integral cross-section including statistical accuracy and detector efficiency determination 2-5%, the normalization accuracy 2.5%, the accuracy of calculation for multiple scattering corrections 2-3%. The uncertainties of initial neutron energy was 5-10 keV.

REFERENCES

1. A. B. Smith, P. T. Guenther, R. D. McKnight, Nuclear Data for Science and Tech., Proc. of Inter. Conf. Antwerp, 1982
2. A. B. Klepatsky, V. A. Konshin et. al. VANT ser. Yadernye Konstanty, 1987, v7, p 3
3. N. V. Kornilov, A. B. Kagalenko et. al. Preprint FEI-2174, 1991
4. A. A. Androsenko, P. A. Androsenko et. al. VANT, ser. Fizika i Tekh. Yadernykh Reaktorov, 1985, v.7, p 33
5. Nuclear Data Stand. for nucl. Meas., IAEA Tech. report 227, Vienn, 1983.
6. N. V. Kornilov, V. Ya. Baryba, O. A. Salnikov Proc. of the 5 All-Union Conf., Kiev, 1980
7. M. Baba, H. Wakabayashi et. al. Jour. of Nucl. Scien. and Tech. 1990, 27(7), p601
8. P. A. Androsenko, VANT sr. Fizika i Tekhn. Yadernykh Reaktorov, 1985, v7, p 45
9. L. P. Abagyan, N. O. Bazazyanc, M. N. Nikolaev, A. M. Tsybula, Group Const. for Reactor and safety calculations, Energoatomizdat, 1981

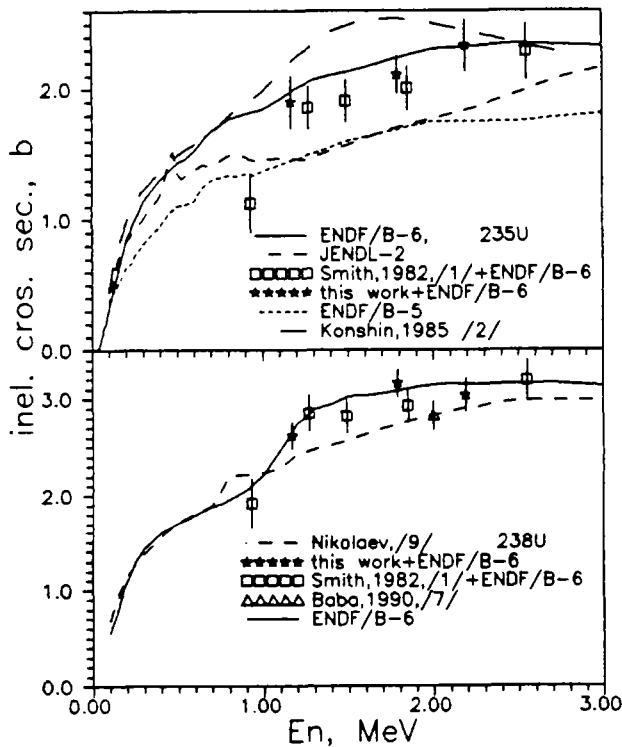


Figure 3. ^{235}U and ^{238}U inelastic neutron scattering cross-sections.

Table 1. Inelastic scattering cross-sections.

| E_0 , MeV | $E_1 - E_2$, MeV | nuclide | σ_{exp} , mb/ster | $\sigma_{in exp}$, b | σ_{lev} | $\sigma_{in tot}$, b |
|-------------|-------------------|------------------|--------------------------|-----------------------|----------------|-----------------------|
| 1.17 \pm | 0-1.04 | ^{235}U | 193.9 \pm 16 | 1.38 \pm 0.2 | 0.520 | 1.90 |
| 0.012 | 0-0.94 | ^{238}U | 110.1 \pm 11 | 1.35 \pm 0.14 | 1.263 | 2.62 |
| 1.79 \pm | 0-1.55 | ^{235}U | 257.0 \pm 11 | 1.54 \pm 0.14 | 0.569 | 2.11 |
| 0.014 | 0-1.55 | ^{238}U | 238.7 \pm 11 | 2.37 \pm 0.14 | 0.784 | 3.16 |
| 2.19 \pm | 0-1.95 | ^{235}U | 309.3 \pm 16 | 1.80 \pm 0.20 | 0.526 | 2.33 |
| 0.015 | 0-1.95 | ^{238}U | 264.5 \pm 14 | 2.46 \pm 0.17 | 0.580 | 3.04 |

NEW DATA ON PREFISSION NEUTRONS FROM 14.7 MeV
NEUTRON-INDUCED FISSION

G.S. Boykov¹, V.D. Dmitriev¹, G.A. Kudyaev², Yu.B. Ostapenko²,
M.I. Svirin², G.N. Smirenkin²

1. V.G. Khlopin Radium Institute, Leningrad, USSR
2. Institute of Physics and Power Engineering, Obninsk, USSR

Abstract: Using time-of-flight technique neutron spectra from 2.9 and 14.7 MeV neutron-induced fission of ^{232}Th , ^{235}U , ^{238}U and ^{237}Np have been measured. The experimental evidence of non-equilibrium neutron emission prior to fission has been obtained. The results of analysis of neutron spectra for the multiple-chance fission made in the framework of statistical model, which take into account the equilibrium and non-equilibrium neutron emission, are presented.

(^{232}Th , ^{235}U , ^{238}U , ^{237}Np , neutron spectra, fission, emission, time-of-flight technique, statistical model)

Introduction

In this paper we report on the results of our neutron spectra measurements and consider some improvements in description of multicomponent fission neutron spectra. The data on fission neutron spectra are of particular importance for applied purposes and development of theoretical description of neutron emission mechanisms.

In accordance with now available data in the case of the first chance fission (it means $E_n < 6$ MeV) the fission neutron spectrum is determined mainly by neutron emission from accelerated fragments. The contribution of other possible mechanisms (such as so-called "scission" neutrons, neutrons emitted during fission fragment acceleration, etc.) is not significant. Although the analysis of numerous experiments has shown that neither Maxwell nor Watt type distributions do not provide the absolutely accurate reproducing of experimental spectra, the deviations are not so remarkable and both of them are commonly used to describe and compare the fission neutron spectra parameters and their behaviour via incident neutron energy.

At incident neutron energies $E_n > 6$ MeV, the shape of neutron spectrum essentially differs from Maxwell or Watt distributions due to significant contribution of neutrons emitted prior to fission. In this energy region the experimental data on fission neutron spectra are limited in number and quality and most of them were taken with insufficient accuracy. Due to these reasons the present status of knowledge about features of neutron emission in the case of the multiple-chance fission is not satisfactory. Some efforts to investigate this topic with use of pure theoretical description in the frame of statistical approach were made by Nix and co-workers [1] and Marten et al. [2]. Despite the remarkable progress achieved in the refinement in the theoretical modeling, there remain open questions

which are important to understanding of the pre-fission neutron emission mechanisms. It might be reasonable to continue both theoretical and experimental study of fission neutron spectra in this field.

Experimental arrangement

Measurements of fission neutron spectra were performed using time-of-flight technique at Radium Institute NG-400 facility. Primary neutrons with energies 2.9 and 14.7 MeV were obtained as a continuous beam in $\text{D}(d,n)$ and $\text{T}(d,n)$ reactions. In order to carry out these measurements we used 4-sectional multilayer ionization chambers to signal the occurrence of fission events (each section incorporates 12 layers with $2\text{mg}/\text{cm}^2$ in thickness and 100 mm in diameter). The gross weight of the isotope under analysis was about 5 g. Each section being connected with separate time-of-flight channel. The fourth "monitor" section contained two targets made of the isotope under analysis with the isotope ^{252}Cf uniformly embedded in them. Thus, fission neutron spectra measurements were made with respect to standard spectrum of ^{252}Cf and both spectra were measured simultaneously. The identity of all sections for count and amplitude characteristics was tested by measuring fission fragment spectra.

The neutron detector (stilbene monocrystal, 10 cm in diameter and 4 cm thick) was housed in a massive shield and located at an angle 90 degrees at flight path length 2.05 m. The overall timing resolution was 2.5 ns. To reduce gamma-quanta background the pulse-shape discriminator with suppression coefficient about 180 for the threshold about 200 keV for neutrons was employed. The additional analysis of neutron detector pulse amplitude was carried out with an aim to decrease the random coincidence background in the range of

low neutron energies. Time-of-flight spectra were corrected for the effects of distortion due to finite energy resolution and differences in flight path for each section of fission chamber. In our measurements background was entirely time independent and its magnitude could be estimated unambiguously. The detailed description of the experimental arrangement was presented earlier /3/.

Experimental data and analysis

The characteristics of the fission neutron spectrum of ^{252}Cf have a status of standards /4/, and being used, the neutron detection efficiency, neutron spectra themselves and integral fission neutron yields can be determined from the results of measurements.

The results of our measurements are shown in Fig.1 in the form of the ratio $R(E)$ of measured spectra $N_1(E, E_n)$ to the reference spectrum $N_{\text{Cf}}(E)$. The

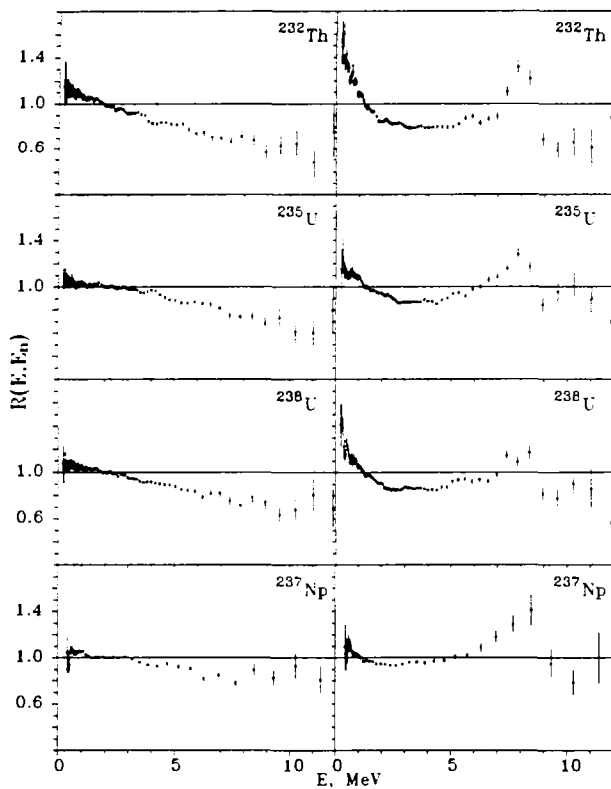


Fig.1. Ratios of spectra $R(E, E_n)$ for ^{232}Th , ^{235}U , ^{238}U , ^{237}Np versus neutron energy E for $E_n = 2.9$ MeV (on the left) and $E_n = 14.7$ MeV (on the right).

characteristics of measured spectra are presented also in the Table 1. As shown in Fig.1, in the case of $E_n = 2.9$ MeV these ratios are practically straight lines. It means that the shape of neutron spectra are very close to Maxwell distribution and the slope of lines is determined by temperatures difference $T_{\text{Cf}} - T_1$.

At 14.7 MeV incident neutron energy the shape of fission neutron spectra is quite different due to neutron emission prior to fission. The contribution of pre-fission neutrons is clearly identified by the deviation from the Maxwell type distribution corresponding to neutron emission from fission fragments. There are some features in the fission neutron spectra. The rise at $E < 2$ MeV is due to evaporative part of pre-fission neutron spectrum, and the maximum at $E \approx 6$ MeV is connected with the non-equilibrium one. Its right slope corresponds to pre-equilibrium spectrum cutting-off by the threshold of residual nucleus fission. At energy range $E < 5$ MeV our data are in a good agreement with previous measurements carried out at incident neutron energy $E_n = 14.3$ MeV /5/.

The last one were satisfactory described with use of simple superposition of Watt and Weisskopf distributions. It is clear now that the high energy part of neutron spectrum is of great importance for understanding of the fission process and the traditional empirical approaches must be refused in favor of a more sophisticated theoretical analysis.

Some improvements have been made to describe the fission neutron spectra /6/. It was shown to achieve a reasonable agreement with experimental neutron spectra measured at $E_n = 14.7$ MeV the partial fission cross-sections must be calculated with high accuracy.

To describe the energy dependence of the fission cross-section $\sigma_f(E_n)$ (including the behaviour of the separate chances) we used:

- the pre-equilibrium neutron emission and Hauser-Feshbach statistical model calculations performed by using a version of the code STAPRE /7/, where neutrons penetrabilities were taken from /8/, the pre-equilibrium neutron emission was calculated with use of exciton model /9,10/;
- the calculations of potential energy and level density as a function of nuclear deformation made on basis of /11/;
- the adiabatic description of collective enhancement of level density /12,13/.

At present time the description of the neutron spectra in the case of the multiple-chance fission of $^{235}\text{U}(n, f)$ and $^{238}\text{U}(n, f)$ has been done /6/. For example the neutron spectra from $^{238}\text{U}(n, f)$ calculated at different incident neutron energies are shown in Fig.2. A good agreement with experiment in the most part of the fission neutron spectra (including the non-equilibrium emission) was obtained. At the same time, there is an excess of neutrons in the low energy part of spectra which can not be reproduced in the frame of our description.

Table 1. Characteristics of measured spectra.

| Target | E_n, MeV | \bar{E}, MeV | T, MeV | $\bar{\nu}$ |
|-------------------|-------------------|-----------------------|-------------------|-----------------|
| ^{232}Th | 2.9 | 1.93 ± 0.03 | 1.285 ± 0.018 | 2.27 ± 0.06 |
| | 14.7 | 1.87 ± 0.03 | | 3.92 ± 0.09 |
| ^{235}U | 2.9 | 2.02 ± 0.03 | 1.344 ± 0.015 | 2.77 ± 0.07 |
| | 14.7 | 2.01 ± 0.03 | | 4.39 ± 0.11 |
| ^{238}U | 2.9 | 2.00 ± 0.03 | 1.332 ± 0.016 | 2.71 ± 0.07 |
| | 14.7 | 1.96 ± 0.03 | | 4.25 ± 0.10 |
| ^{237}Np | 2.9 | 2.05 ± 0.03 | 1.369 ± 0.010 | 2.98 ± 0.07 |
| | 14.7 | 2.11 ± 0.03 | | 4.45 ± 0.08 |

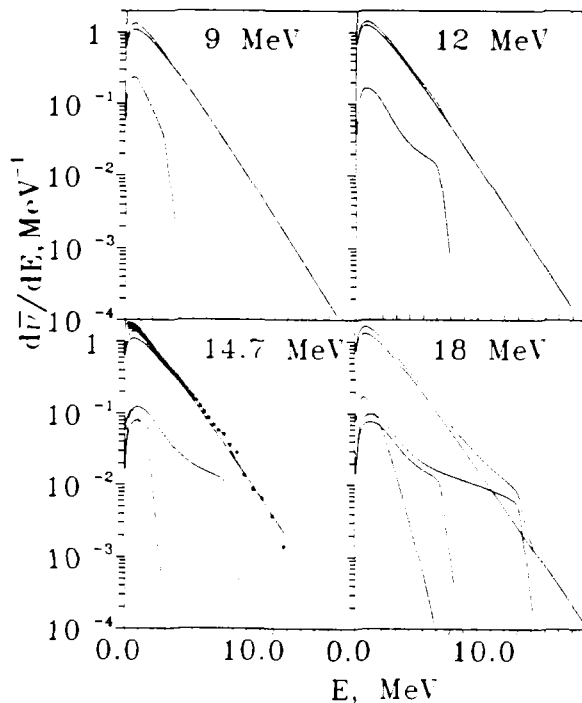


Fig.2. The neutron spectra from $^{238}\text{U}(n,f)$ reaction at different incident neutron energy. The points represent data of our measurements. The solid lines are the results of calculations.

The yields of this "additional" pre-fission neutrons are 0.3 both for ^{235}U and ^{238}U and their spectra can be described with use of Weisskopf distribution with the temperature $\tau \approx 0.4$ MeV. Up to now we have no any reasonable explanation for this effect.

References

1. D.G. Madland, R.J. LaBauve, J.R. Nix, Proc. of an IAEA Consult. Meeting on Physics of Neutron Emission in Fission, Mito, Japan, 1988, Vienna, 1989, p.259.
2. H. Marten, A. Ruben, D. Seeliger, *ibid*, p.245.
3. G.S. Boykov, V.D. Dmitriev, G.A.

- Kudyaev et al., Proc. of Int. Conf. "50-th Ann. of Nucl. Fiss.", Leningrad, USSR, 1989; Atomnaya Energiya, 1990, v.69, p.23.
4. 1982 INDC/NEANDC Nuclear Standards File, Tech.Rep. No.277, IAEA, Vienna, 1983.
5. Yu.A. Vasil'ev et al., JETP, 1960, v.38, p.671.
6. G.S. Boykov, V.D. Dmitriev, G.A. Kudyaev et. et al., Yadernaya Physica, 1991, v.53, p.628; G.S. Boykov, V.D. Dmitriev, G.A. Kudyaev et al., Z.Phys.A (to be published).
7. M. Uhl, B. Strohmer, Report IPK-76/01, Vienna, 1976, Addenda, 1978.
8. Ch. Lagrange, Report INDC(Fr)-56/L (NEANDC-228-L), 1982.
9. M. Blann, Phys.Rev.Lett., 1970, v.21, p.1357; v.22, p.337; Ann. Rev. Nucl. Sci., 1975, v.25, p.1231.
10. A.V. Ignatyuk, V.M. Maslov, A.B. Paschenko, Yadernaya Physica, 1983, v.47, p.355.
11. V.V. Pashkevich, Nucl.Phys.A, 1971, v.169, p.275; Int.School-Seminar on Heavy Ion Physics, Alushta, 1983, Dubna, 1983, p.405.
12. S. Bjornholm, A. Bohr, B.R. Mottelson, Phys. and Chem. of Fission (Proc.Simp., Rochester, 1973), Vienna, IAEA, 1974, v.1, p.361.
13. G.A. Kudyaev, Yu.B. Ostapenko, G.N. Smirenkin, Yadernaya Physica, 1987, v.45, p.1534.

ROTATIONAL MODES CONTRIBUTION TO THE OBSERVED LEVEL DENSITY

E.M. Rastopchin, M.I. Svirin, G.N. Smirenkin

Institute of Physics and Power Engineering, Obninsk, USSR

Abstract: Attempt is made to apply the level density systematics within the framework of the generalized superfluid model to the $A < 150$ region. The analysis of some properties of these nuclei (e.g deformation energy, neutron resonance density, neutron evaporation spectra) shows the existence of large groups of nuclei, for which the contribution of rotational modes to their level density is considerable (in spite of the traditional classification according to low-lying discrete level spectra).

(statistical model, level density of excited nuclei, collective enhancement factor, neutron resonance density, evaporation neutron spectra, low-lying excited levels)

For a long period of time experiments preceded theoretical work in nuclei deformation research. Phenomenological analysis of various spectroscopic characteristics led to the discovery of two nuclei regions, the lantanides and the actinides, with spheroidal form and quadrupole deformation $\epsilon \approx 0.2-0.3$. Theory evened up the score with the development of shell correction method [1,2]. It not only revealed the physical nature of nuclei deformation, but also showed that the number of deformed nuclei is much greater than one can find out from properties of systematics of low-lying excited levels. Experimental data concerning higher-lying levels near neutron binding energy B_n confirm the latter statement [3,4]. The present paper also deals with this problem.

freedom to the level density is taken account of by multiplying the internal density of excited nuclei levels by the corresponding enhancement factors (rotational K_{rot} and vibrational K_{vib})

$$\rho(U, J) = \rho_{in}(U, J) K_{col}(U) \quad (1)$$

$$K_{col}(U) = K_{rot}(U) K_{vib}(U) \quad (2)$$

In (1) $\rho_{in}(U, J)$ is described using well-known expression:

$$\rho_{in}(U, J) = \frac{\omega(U)}{\sqrt{8\pi} \sigma^3} (2J+1) \exp\left[-\frac{J(J+1)}{2\sigma_{\perp}^2}\right] \quad (3),$$

where $\omega(U)$ is nuclear state density; $\sigma^3 = \sigma_{sph}^3$, $\sigma_{\perp}^2 = \sigma_{sph}^2$ is the spin cut-off

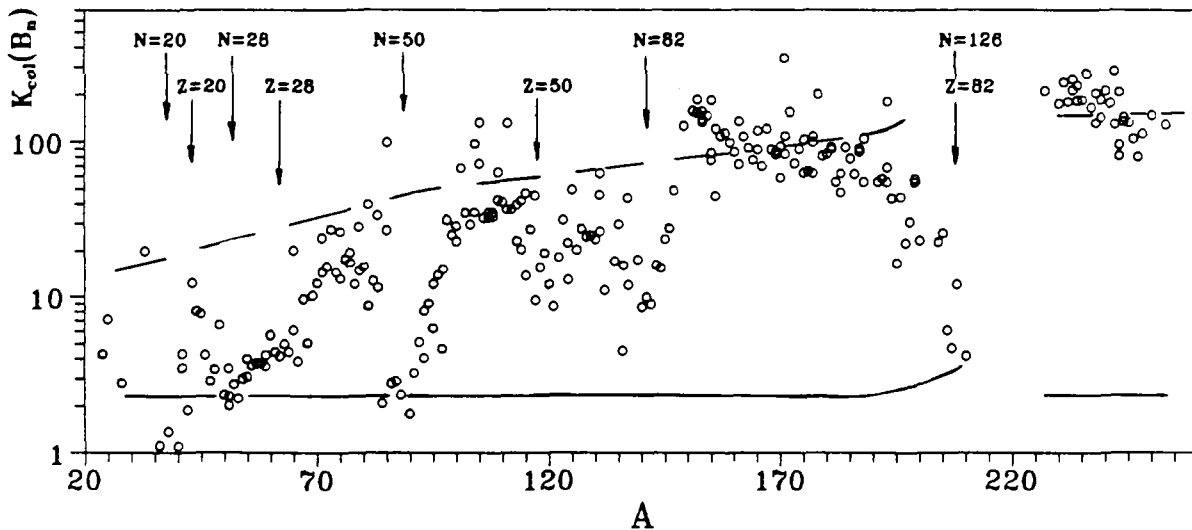


Fig.1 Dependence of the collective enhancement factor $K_{col}(B_n)$ on the mass number A ; where \circ - designates the values, at which the NRD description is made according to GSM systematics [7,9]; solid curve - $K_{col} = K_{vib}$, dashed curve - $K_{col} = K_{vib} K_{rot}$. Arrows show the magic nuclei, which are placed on the β - stability line.

The level density $\rho(U, J)$ for the given excitation energy U and angular momentum J of the nucleus depends upon collective properties of the excited nuclei. In the adiabatic approach [5-7] the contribution of collective degrees of

parameter for spherical nuclei and $\sigma^3 = \sigma_{\perp}^2 \sigma_{\parallel}$, $\sigma_{\perp}^2 = \sigma_{\perp}^2$ - for the deformed ones; $\sigma_i^2 = F_i T$ ($i=1, \parallel$), F_i is the corresponding moment of inertia and T is nuclei temperature.

The rotational enhancement factor for nuclei with spheroidal form can be presented in the following form $K_{rot} = \sigma_1^2$ [5].

If we put $K_{col} = 1$ into (1), then the analysis of the observed neutron resonance density (NRD) leads to a considerable overestimation of the asymptotic (for great U) level density parameter $\tilde{a}(A)$ as compared to the microscopic calculation results (the level density parameter obtained from the single particle energies in a Woods-Saxon potential [6]) $\tilde{a}_{micro}/A = 1/10 + 1/11 \text{ MeV}^{-1}$. In this case the fermi-gas model for $\rho(U, J)$ gives $\tilde{a} \approx A/7 \text{ MeV}^{-1}$, while the superfluid model gives still greater value $\tilde{a} \approx A/5 \text{ MeV}^{-1}$. This discrepancy is eliminated by taking into account the collective modes and in the last variant, named the generalized superfluid model (GSM), one can obtain the value of $\tilde{a} \approx \tilde{a}_{micro}$. This result of GSM systematics proceeds from the NRD analysis for the nuclei with well-defined collective properties: the deformed ones for $A \approx 150-190$ and $A > 230$ ($K_{rot} \gg 1$) and the spherical ones in the vicinity of closed nucleonic shells ($K_{rot} = 1$) [7]. What will happen if all these restrictions concerning the nucleon structure are lifted?

The curves in fig.1 show how the K_{col} description is applied to GSM systematics in two variants:

$$K_{col} = \begin{cases} K_{vib} & \text{for spherical nuclei} \\ K_{rot} K_{vib} & \text{for deformed nuclei} \end{cases} \quad (4)$$

where the upper one is marked by solid curve, and the lower one - by dashed curve. The experimental points $K_{col}^{exp}(B_n)$ in fig.1 correspond to the values of this factor, which represent the observed NRD in GSM systematics. One can see that $K_{col}^{exp}(B_n)$ of magic and near magic (spherical) nuclei are close to the solid curves, while the ones for lanthanides and actinides lie close to the dashed curve as the GSM systematics prescribes. In the most part of $A \leq 150$ region the $K_{col}(B_n)$ values are much greater than one can expect for the spherical nuclei. For $A \approx 70+85$ and $105+125$, K_{col} is closer to $K_{col} = K_{vib} K_{rot}$, just as for the deformed nuclei.

Fig.2 shows the potential energies $V(\epsilon)$ as functions of the quadrupole deformations ϵ for a few representatives of "anomalous" groups of nuclei as well as for the ^{196}Pt nucleus from the transition region between the deformed nuclei (lanthanides) and doubly magic ^{208}Pb . All of them have minima $V(\epsilon)$ at

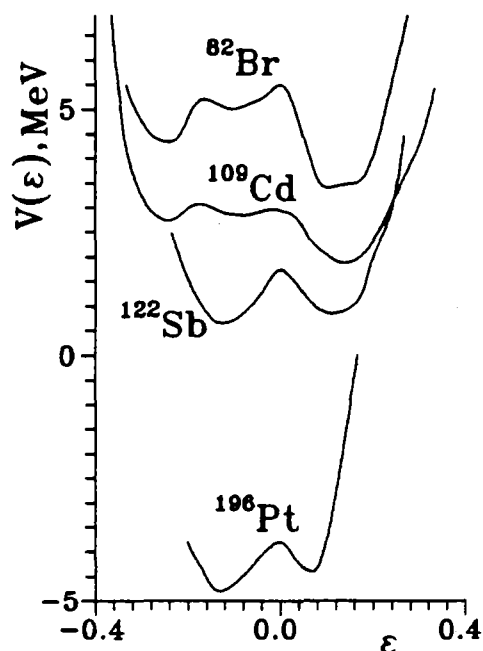


Fig.2 Nuclei deformation potential energies in the vicinity of equilibrium deformations $\epsilon = \epsilon_0$.

$\epsilon \neq 0$ and this fact may be connected with the raised rotational modes contribution to $\rho(U, J)$.

To determine which case is nearer to the real nuclei level density, i.e. what is the rotational modes contribution to it, we can use two more sources of experimental information, examples of which are shown in fig.3 and fig.4. They are: 1) the experimental information of the energy dependence of the nuclei level density, especially when $U \leq B_n$, which is obtained from the evaporation spectra of (p,n) reactions, just as in [3]; 2) the level density of almost cold nuclei, shown in the form of histograms. The latter ones are the numbers of levels per the interval of the excitation energy, calculated with the help of spectroscopic data, e.g. [8], without any spin or parity restriction.

Fig.3 shows that for the residual nucleus ^{109}Cd mutually corresponding NRD information and $^{109}\text{Ag}(p, n)^{109}\text{Cd}$ reaction neutron spectrum match the intermediate case for (4). Experimental data for ^{109}Cd are closer to the ones predicted by GSM systematics for the deformed nuclei, which corresponds qualitatively to the behaviour character of deformation energy $V(\epsilon)$ in fig.2.

Fig.4 demonstrates much more clearly the transition from spherical nuclei to deformed ones in the vicinity of lead. It shows the full level density $\rho_t(U)$ (summed over all angular momenta) according to the GSM systematics (dashed curves) and microscopical calculations (solid curves). We calculated $\rho_t(U)$ just like for the spherical nuclei, so the deviation of experimental data from the calculated curves, which grows as Z and A diminish, can be viewed as evidence of

rotational modes contribution increase. We would like to stress the significance of the discrepancies at low excitation energies when $K_{vib} \approx 1$.

The general case is more complicated. It does not contain such systematized classification of collective and shell properties, as it does in the vicinity of doubly magic ^{208}Pb . Fig.1 shows that in the vicinity of β -stability valley most nuclei ($A < 150$) are far from closed shells either by both sorts of nucleons, or by one of them (in contrast to the nuclei in the vicinity of ^{208}Pb). This fact determines the special character of $A < 150$ region, which cannot yet be put into GSM systematics [7,9]. This region deserves special attention from the practical point of view because it includes most of the actinides fission fragments.

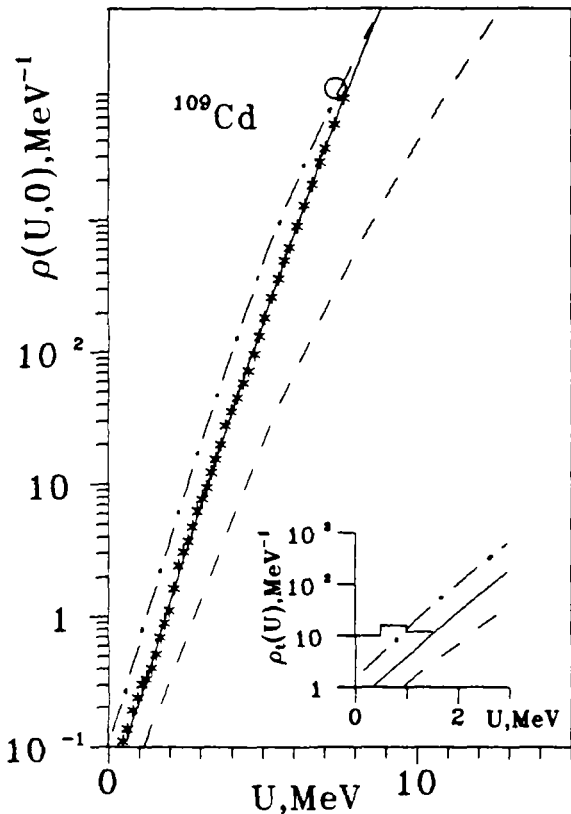


Fig.3 Energy dependence of the level density $\rho(U, J=0)$ for the ^{109}Cd nucleus. $\circ - \rho(B_n, J=0)$ (obtained from NRD), $*$ - and --- from [13], where --- is the GSM calculation of [7] for $K_{rot}=1$; -.-.- is the same for $K_{rot}=0.5$. Insertion: $\rho_t(U)$, the curves are marked just as in the main part, histogram shows the density of low-lying levels [8] (see the text).

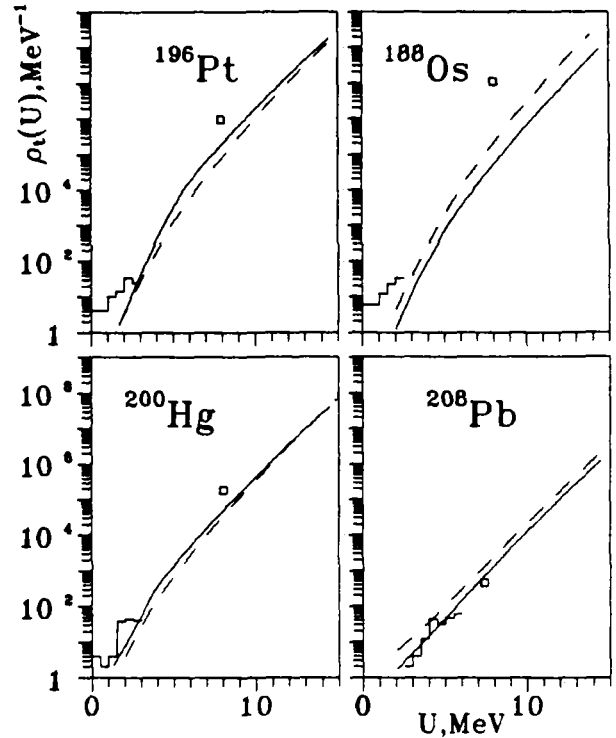


Fig.4 The full (summed over J) level density $\rho_t(U)$. Where --- is microscopic calculation; --- is the GSM systematics [7,9], $\square - \rho_t(B_n)$, (obtained from NRD), the histogram is [8].

References

1. V.M. Strutinsky: Nucl. Phys. 95, 420 (1967); Nucl.Phys. 122, 1 (1968).
2. P. Moller, J.R. Nix: Nucl. Phys. A361, 117 (1981)
3. M.I. Svirin, G.N. Smirenkin: Proc. Int. Conf. on Nucl. Data for Sci. and Technol., Mitto, JAERI, 763 (1988); Yad. Fyz. 48, 682 (1988).
4. E.M. Rastopchin, M.I. Svirin, G.N. Smirenkin: Yad. Fyz. 52, 1258 (1990).
5. S.Bjornholm, A. Bohr, B. Mottelson: In: Physics and chemistry of fission 1973, V.1, p.367. Vienna: IAEA 1974.
6. A.V. Ignatyuk: Statistical properties of excited nuclei, Moscow, Energoatomizdat 1983.
7. A.V. Ignatyuk, K.K. Istekov, G.N. Smirenkin, Yad. Fyz. 29, 875 (1979).
8. C.M. Lederer, V.S. Shirley: Tables of isotopes. N.Y.: J.Wiley and Sons, Inc., 1978.
9. E.M. Rastopchin et. al, Yad. Fyz. 49, 24 (1989).